

## Article

# Bound-State Soliton and Noise-like Pulse Generation in a Thulium-Doped Fiber Laser Based on a Nonlinear Optical Loop Mirror

Maria Michalska <sup>1,\*</sup>, Jakub Michalski <sup>2</sup>, Pawel Grzes <sup>1</sup> and Jacek Swiderski <sup>1</sup>

<sup>1</sup> Institute of Optoelectronics, Military University of Technology, 2 Sylwestra Kaliskiego Street, 00-908 Warsaw, Poland; pawel.grzes@wat.edu.pl (P.G.); jacek.swiderski@wat.edu.pl (J.S.)

<sup>2</sup> Faculty of Mechatronics, Armament and Aerospace, Military University of Technology, 2 Sylwestra Kaliskiego Street, 00-908 Warsaw, Poland; jakub.michalski@wat.edu.pl

\* Correspondence: maria.michalska@wat.edu.pl

**Abstract:** We demonstrate a thulium-doped, mode-locked, all-fiber laser capable of operating in two generation regimes: dispersion-managed soliton and noise-like pulse (NLP). Employing a nonlinear optical loop mirror as an artificial saturable absorber, the oscillator generated optical pulses with a fundamental pulse repetition frequency of ~15.795 MHz. The total net dispersion of the laser cavity had a slightly anomalous group delay dispersion value of  $-0.016 \text{ ps}^2$ . After appropriate adjustment of a polarization controller, bound states of a dispersion-managed soliton composed of three pulses with fixed soliton separations were also observed. NLP generation, tunable over 35 nm from 1943.5 to 1978 nm, was also presented in the same laser setup. To our knowledge, this is the first report of the generation of tunable NLPs in a mode-locked thulium-doped fiber laser based on a nonlinear loop mirror saturable absorber.

**Keywords:** thulium-doped fiber laser; bound-state soliton; noise-like pulse; nonlinear optical loop mirror



**Citation:** Michalska, M.; Michalski, J.; Grzes, P.; Swiderski, J. Bound-State Soliton and Noise-like Pulse Generation in a Thulium-Doped Fiber Laser Based on a Nonlinear Optical Loop Mirror. *Appl. Sci.* **2022**, *12*, 1664. <https://doi.org/10.3390/app12031664>

Academic Editor: Manuel Armada

Received: 5 January 2022

Accepted: 3 February 2022

Published: 5 February 2022

**Publisher's Note:** MDPI stays neutral with regard to jurisdictional claims in published maps and institutional affiliations.



**Copyright:** © 2022 by the authors. Licensee MDPI, Basel, Switzerland. This article is an open access article distributed under the terms and conditions of the Creative Commons Attribution (CC BY) license (<https://creativecommons.org/licenses/by/4.0/>).

## 1. Introduction

An intense development of low-loss fiber components for operation in the 2  $\mu\text{m}$  wavelength region has yielded the rapid progress of mode-locked all-fiber lasers emitting in this spectral region. Broadband ultrafast fiber lasers delivering pico- and femtosecond pulses have attracted significant interest in the research community because of their wide range of applications including spectroscopy, medicine, material processing, remote sensing, optical communications, nonlinear conversion, and supercontinuum generation [1]. Owing to the wide and smooth emission spectrum of  $\text{Tm}^{3+}$  ions in silica, mode-locked Tm-doped fiber lasers (TDFLs) are very attractive and one of the most commonly used choices for the generation of ultrashort pulses at a wavelength of 2  $\mu\text{m}$ . However, the generation of ultrafast femtosecond optical pulses requires dispersion management of the laser cavity because most single-mode silica fibers and fiber components exhibit anomalous dispersion in the 2  $\mu\text{m}$  spectral region. When the total net dispersion is close to zero, a dispersion-managed soliton (i.e., stretched-pulse) with a large spectral bandwidth and short pulse duration after compression can be generated [2–6]. This mode-locking regime enables a shorter femtosecond pulse generation compared with soliton mode-locking. The two shortest stretched-pulses with durations of 119 fs and 173 fs were generated in non-fully fiberized TDFLs mode-locked by nonlinear polarization rotation (NPR) [4,5]. However, ultrashort pulses with durations of ~200 fs and 253 fs emitted from all-fiber laser setups have also been reported [2,6].

Near-zero cavity net dispersion, under strong pumping multiple dispersion-managed solitons, can be generated in a passively mode-locked fiber laser. When two or more

fundamental solitons circle in the laser cavity, they propagate with the same velocity and can form a bound state. Bound states of solitons have been firstly studied numerically as high-order soliton solutions of the nonlinear Schrodinger equation [7,8]. The first experimental demonstration of its generation in a fiber laser was reported in 2001 in an Er-doped ring fiber laser [9]. Then, bound states of solitons were reported and intensively investigated in fiber lasers with different total net dispersion—the large normal and anomalous cavity dispersion as well as in a dispersion-managed fiber laser with near-zero cavity net dispersion [10–14]. In 2019, bound solitons with tunable spectral bandwidth and pulse width as well as soliton separation were demonstrated in an Er-doped fiber laser with normal net dispersion [13]. Bound states have been also described in the 2  $\mu\text{m}$  wavelength region in TDFLs with slightly anomalous net dispersion and mode-locked by NPR [14]. These specific types of ultrashort pulses with fixed separations might be applied in optical communication to enlarge the data-carrying capacity of fiber link [15,16]. However, reports on bounded solitons in the 2  $\mu\text{m}$  wavelength region are still sparse.

Another mode-locking regime, which enables the generation of an optical pulse trace with a relatively high average output power and high pulse packet energy, is noise-like pulse (NLP) generation. This mode-locking operation commonly occurs in different types of passively mode-locked fiber lasers independently of laser cavity dispersion. NLP generation, characterized by a smooth and broad optical spectrum [17–22], is a packet of multiple ultrashort pulses with randomly varying intensities and durations inside a longer envelope [22]. Owing to their relatively high output power, they are capable sources for various applications that do not require highly coherent pulses, such as supercontinuum generation, material processing, or low-coherence interferometry and sensing [23–26]. Furthermore, NLPs can also be used in data storage, optical communications, or temperature profile measurements [27–29]. In TDFLs, NLPs with a high bunch energy of 249 nJ (377 mW average power at a repetition rate of 1.514 MHz [18]) and a high average power of 730 mW [19] have been reported. The broadest NLP spectrum with a 300 nm bandwidth at 10 dB level, was generated in the TDFL with normal dispersion [20].

In this paper, we report the demonstration of two types of dispersion-managed solitons, i.e., stretched-pulse and bound states solitons, generated in a thulium-doped all-fiber laser using a nonlinear optical loop mirror (NOLM) as a saturable absorber. In addition, at a higher pump power level, NLP generation tunable over 35 nm from 1943.5 to 1978 nm was also presented in the same laser setup. Spectral tuning was realized by a very simple, fast, and cost-effective method which does not require any expensive optical component. A proper adjustment of the polarization controller position enabled a wavelength shift. The maximum generated NLP energy was 2.91 nJ.

## 2. Materials and Methods

A schematic of the Tm-doped fiber laser setup mode-locked by a NOLM is shown in Figure 1 and has been described in a previous paper [6]. The proposed oscillator consists of two loops combined by a  $2 \times 2$  fused polarization-maintaining (PM) fiber coupler with a splitting ratio of 90:10. A 0.14 m-long PM, highly thulium-doped fiber (Coherent, PM TSF-5/125) was used as the gain medium in the main loop. The active fiber was pumped in a co-propagation scheme through a 1560/2000 wavelength-division multiplexing (WDM) coupler by a home-built Er/Yb-co-doped all-fiber laser (EYDFL) with a continuous-wave (CW) output power of up to 1.6 W at 1564 nm. A polarization-sensitive fiber optic isolator (ISO) was used to ensure unidirectional operation. The output coupler (OC) was a  $1 \times 2$  PM fiber coupler that extracted 30% of the intracavity power.

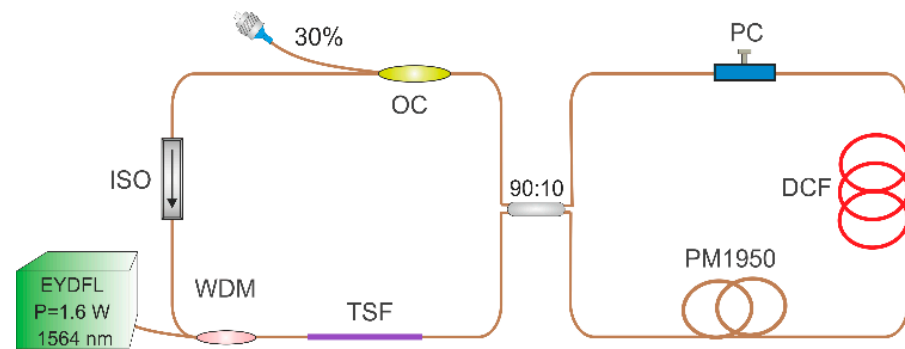


**Figure 1.** Experimental setup of the mode-locked TDFL with NOLM; EYDFL—Er/Yb-co-doped ring fiber laser, WDM—1560/2000 wavelength division multiplexer, TSF—single-mode thulium-doped fiber, OC—output coupler, ISO—fiber optic isolator, PM1950—PM passive fiber, DCF—dispersion compensation fiber, PC—polarization controller.

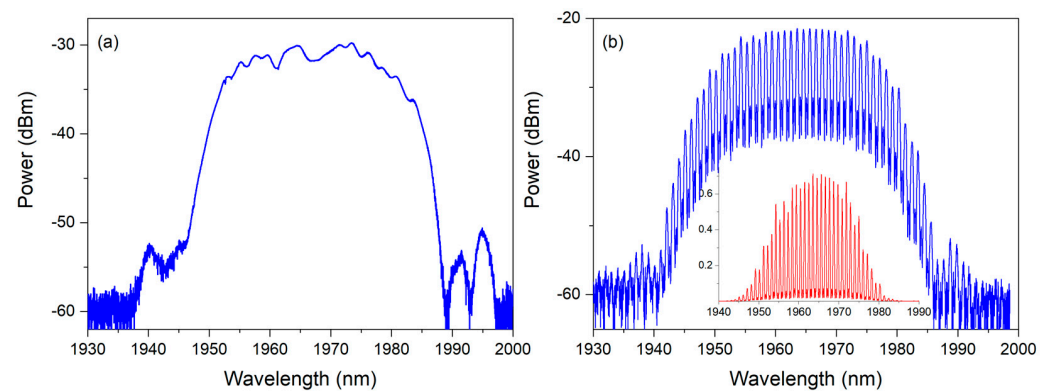
The right loop of the developed TDFL acts as a fast artificial saturable absorber (NOLM). This nonlinear fiber loop, which is based on the optical Kerr effect, causes a phase-shift difference for counter-propagating pulses in the loop [30]. The counter-propagating pulses interfere with each other during propagation through the central fiber coupler, and hence the transmission of the loop depends on the amplitude of the pulse launched into the NOLM, the loop length, and the asymmetric splitting ratio of the fiber coupler [31]. Almost the entire laser cavity was fusion-spliced using single-mode, PM, PANDA-style fibers and components. A single-mode, non-PM, ultra-high numerical-aperture fiber (UHNA4) with a core/clad diameter of 2.2/125  $\mu\text{m}$ , numerical aperture of  $\text{NA} = 0.35$ , and group velocity dispersion of  $\beta_2 = 93 \text{ ps}^2 \text{ km}^{-1}$  [32] was employed as a dispersion compensation fiber. This was the only non-PM component in the entire oscillator setup. Apart from the dispersion-compensation fiber (DCF), a passive, anomalous-dispersion PM1950 fiber was used in the NOLM to ensure a sufficient phase shift difference between the counter-propagating pulses in the loop for a stable mode-locking operation.

Owing to the large difference in the mode field diameters between the small-core UHNA4 fiber and the PM1950, a thermal core expansion method [33] was adopted for fiber joint formation. After optimization of the filament fusion-scanning process across the splice joint, a laser power transmission of 89% was achieved for the light propagation from the PM1950 (7.2  $\mu\text{m}$  core diameter) to the UHNA4 (2.2  $\mu\text{m}$  core diameter) fiber. An in-line polarization controller (PC) inserted onto the DCF was employed to adjust the intracavity polarization state and start the mode-locking operation. In the experiment, the DCF was 5.58 m long. The entire length of the laser cavity was  $\sim 13.2$  m, while the total net dispersion was adjusted to  $-0.016 \text{ ps}^2$ .

### 3. Results and Discussion

Figure 2 shows the output spectra of the dispersion-managed solitons generation from the developed TDFL for different PC positions. All spectra were measured using an optical spectrum analyzer (AQ6375, Yokogawa Tokyo Japan) with a resolution bandwidth of 0.1 nm. The spectrum shown in Figure 2a corresponds to a stretched-pulse generation. It is centered at a wavelength of 1967 nm and characterized by a full width at half maximum (FWHM) bandwidth of 24.7 nm. For 560 mW of pump power, the oscillator provided stable single-pulse CW-mode-locking operation with an average output power of 0.9 mW and a fundamental pulse repetition frequency of 15.795 MHz, which corresponded to the round-trip time of the laser cavity. This mode-locking operation, obtained after careful PC position adjustment, has been presented and discussed in M. Michalska's previous work describing intracavity dispersion management in this TDFL setup [6]. In that paper, the soliton mode-locking and the generation of a dispersion-managed soliton were presented and discussed. Using different lengths of DCF in the NOLM, a mode-locking operation in the laser cavity with total net dispersion ranging from  $-0.016 \text{ ps}^2$  to  $-1.149 \text{ ps}^2$  was

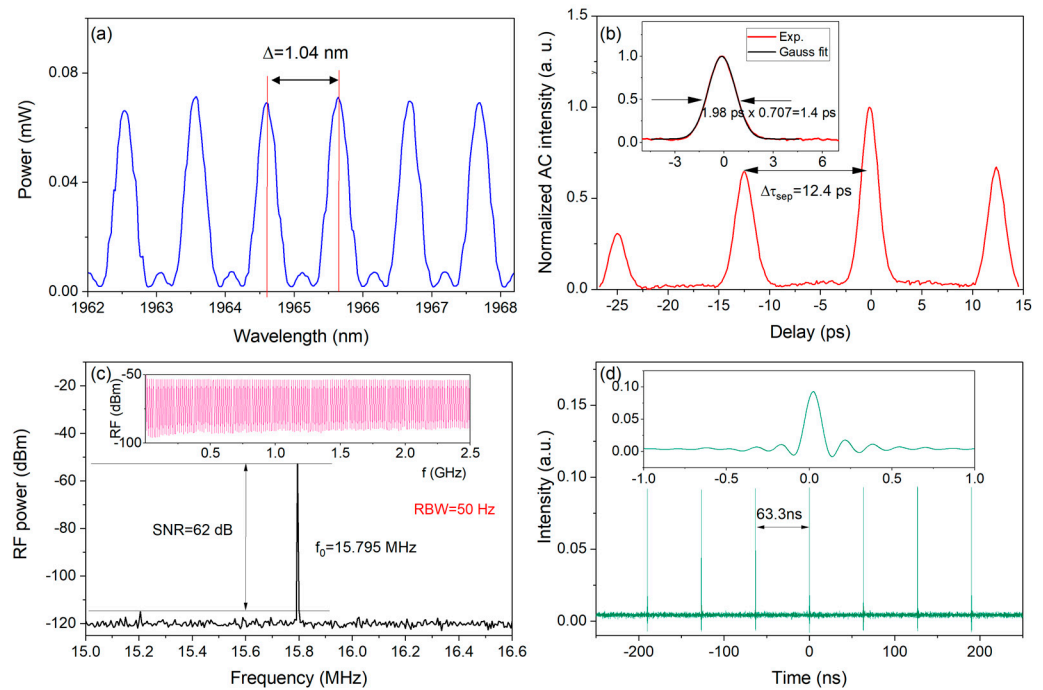
obtained. Laser output pulses were positively chirped and, therefore, stretched in time. In the stretched-pulse mode-locking regime, the shortest laser pulses with Gaussian shape and a duration of 1.56 ps, compressed in the PM, single-mode fiber to 253 fs, were obtained.



**Figure 2.** Optical spectra of dispersion-managed solitons: (a) stretched-pulse generation; (b) bound-state soliton generation mode; the inset presents the same optical spectrum in the linear scale (red trace).

Figure 2b shows the generated optical spectrum of bound states of soliton. This spectrum was obtained for different PC positions and for a pump power of 513 mW. The bound states of soliton were measured at a slightly lower pump power than that applied for stretched-pulse generation, because it is affected by the PC position setting. The output spectrum, generated during the stable CW mode-locking operation, appeared centered at 1964.2 nm and characterized by a 21.9 nm spectral bandwidth at  $-3$  dB level. It exhibited characteristic modulated fringes, as a result of spectral interference among solitons with small temporal intervals. The formation of multiple solitons in the laser cavity is caused by a peak power clamping effect [34]. Peak power clamping was induced in our laser by a sinusoidal transmission of the NOLM and made solitons stable in the cavity with a strong laser gain. The adjustment of the PC position changed the linear phase delay between two orthogonal polarization components in the cavity. For a certain linear cavity phase delay, a propagating soliton with a high peak power can generate such a high nonlinear phase shift that it switches the cavity feedback, which limits the soliton peak power. When the peak power is clamped, the high laser gain supports the formation of additional solitons with the same amplitude and pulse duration.

In Figure 3a, part of the output spectrum of bound solitons spanning from 1962 to 1968 nm is displayed. The spectral lines are equidistantly spaced in the whole spectrum by  $\sim 1.04$  nm. Figure 3b presents the autocorrelation measurement results obtained using the interferometric autocorrelator Femtochrome FR 103MC, USA. In the AC trace, four pulses separated by the time interval of 12.4 ps are present, which is consistent with a spectral modulation period of 1.04 nm. The peaks in the AC trace can be fitted with Gaussian shape, and the FWHM pulse duration of each peak is  $\sim 1.98$  ps, corresponding to the FWHM pulse durations after deconvolution of 1.4 ps. The pulse interval is 6.3 times the pulse width. By analyzing the AC measurement results, it can be concluded that the three dispersion-managed solitons were bound. However, the autocorrelation signal associated with bound-state soliton generation was longer than the available measurement time window of our autocorrelation system software. A complete AC trace should contain one more pulse on the right side, which is not present in Figure 3b due to the limitations of our measurement equipment. The intensity ratio of the peaks in the autocorrelation trace was 1:2:3:2, and an intensity ratio of 1:2:3:2:1 corresponds to propagation of three solitons in bound states with identical amplitude and equal pulse separation [9]. The average output power of this bound-state soliton was 1.42 mW, which corresponds to a pulse energy of each solitons of  $\sim 30$  pJ. For a higher pump power, the fill factor of the spectrum of the generated bound-state solitons decreased, and multi-pulse mode-locking operation occurred.



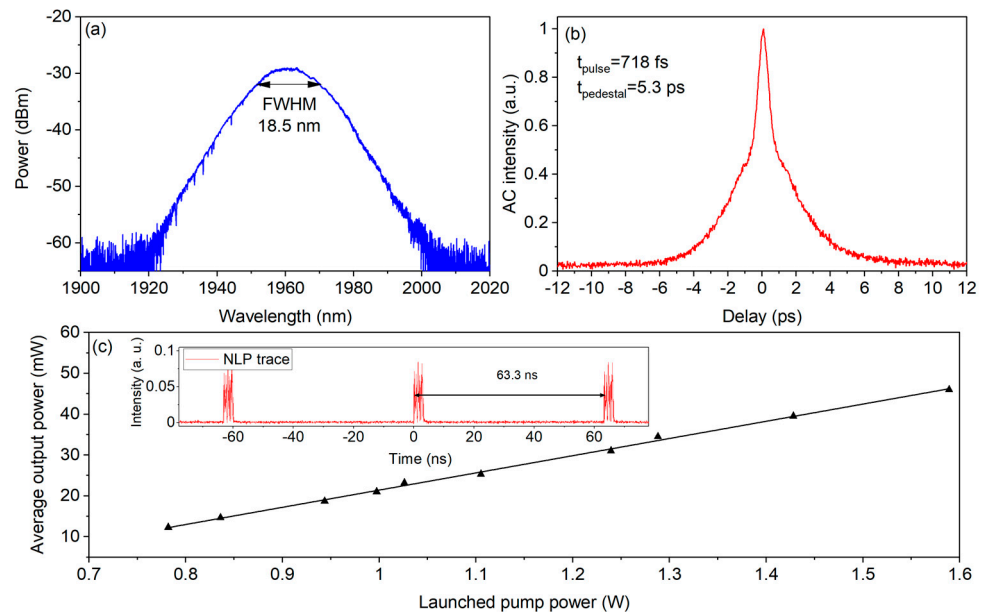
**Figure 3.** Output characteristics of the bound-state soliton generation mode: (a) part of the output spectrum of bound solitons spanning from 1962 to 1968 nm; (b) autocorrelation trace (c) radio-frequency spectrum with scanning ranges of 1.6 MHz and 2.5 GHz (inset), and (d) oscilloscope trace of the mode-locked pulse train (inset: single pulse).

Figure 3c displays the radio frequency (RF) spectrum of the generated bound states of the solitons. It was measured using an RF spectrum analyzer (Keysight Technologies N9918A, Malaysia) with a resolution bandwidth of 50 Hz. The measured repetition rate of 15.795 MHz confirmed that the oscillator operated at the fundamental pulse repetition frequency resulting from the cavity length. The signal-to-noise ratio (SNR) of the fundamental frequency was approximately 62 dB. This is a better result than those previously reported for TDFLs [11,12,14]. The RF spectrum measured in the long-range frequency span (0–2.5 GHz), presented as an inset in Figure 3c, did not contain any modulations and confirmed a stable, mode-locking operation.

Figure 3d presents a pulse train generated during mode-locking operation yielding bound solitons and measured using a sampling digital oscilloscope with a 6 GHz bandwidth, 25 GSa/s sampling rate (DSA 70604, Tektronix, Beaverton, OR, USA), and a fast photodetector with a rising time of less than 35 ps (ET-5000F, EOTech, Traverse City, MI, USA). The inset depicts a single pulse recorded by an oscilloscope with a typical sinc function shape. Oscilloscope traces showed single-pulse mode-locking operation, and bound states of solitons cannot be noticed in Figure 3d because the time during which the solitons which were bound was too short to be measured by our photodetector.

By adjusting the PC at a higher pump power level (mostly at a pump power of 1 W), an NLP operation mode was realized in the developed TDFL. An adjustment of the PC shifts the cavity phase delay, and the soliton operation is tuned into the mode-locking operation where a laser pulse consists of a bunch of ultrashort pulses. The formation of noise-like pulse was found to be connected with the soliton collapse effect [35]. In the laser cavity when the pulse peak power is unclamped (different PC position), the soliton peak power increases with the increase of pump power. As a result, the pulse duration decreases, and the soliton spectrum broadens so that it becomes comparable with the gain bandwidth of the active fiber. Then, the soliton experiences a sudden losses and collapses. When the soliton collapses, a new pulse is built up from the collapsed one. The process is repeated and, because of gain competition, a bunch of ultrashort pulses with randomly varying intensity and pulse duration is created.

In Figure 4a, a typical broad and smooth NLP spectrum with FWHM bandwidth of 18.5 nm is presented. The output spectrum is centered at 1961.4 nm. An NLP packet was generated with the same fundamental frequency as that of dispersion-managed solitons of 15.795 MHz. Mode-locked NLPs were generated in a variety of intracavity polarization states (for different positions on the PC). A change in the PC position led to optical spectrum tuning, which is presented in Figure 5 and is discussed in the next part of this paper.



**Figure 4.** Noise-like pulse generation characteristics: (a) optical spectrum and (b) autocorrelation trace for 46 mW of average output power; (c) average output power as a function of the pump power launched into the TDF; the inset shows the oscilloscope trace of the NLP train.

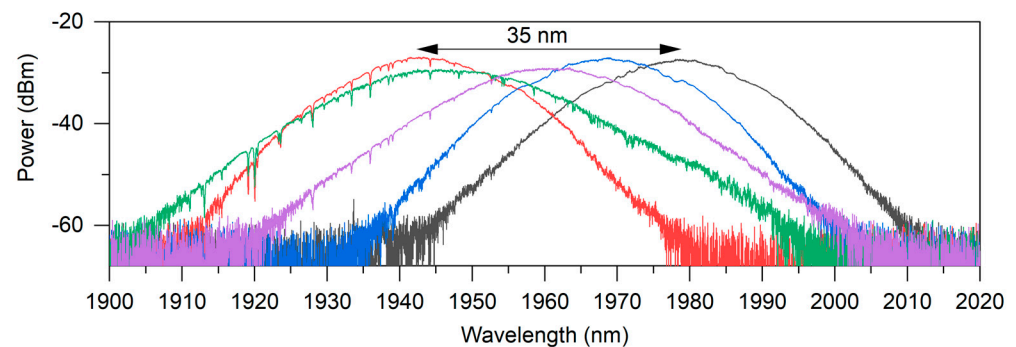


**Figure 5.** NLP output spectrum tuning at a pump power of 1.3 W.

As shown in Figure 4c, the output power of the generated NLP increased linearly with the increase of the pump power. The maximum average output power was 46 mW at an incident pump power of 1.59 W, and the slope efficiency was  $\sim 4.2\%$ . The minimum pump power required to support NLP generation was 0.78 W. It is believed that by applying a more powerful pump source, the NLP output power can be easily scaled up to hundreds of milliwatts. For the maximum pump power, the oscillator generated NLP packets with a duration of 3 ns and the same fundamental pulse repetition frequency of 15.795 MHz. The calculated maximum NLP energy was 2.91 nJ. At the recorded autocorrelation trace shown in Figure 4b, a narrow peak on the broad pedestal could be observed, which is typical for noise-like generation. The autocorrelation spike had an FWHM duration of 718 fs and a pedestal FWHM of 5.3 ps. The autocorrelation spike could be fitted with a Gaussian pulse profile, and then FWHM spike duration was determined to be 509 fs. The intensity ratio of the pedestal to the peak was approximately 0.5.

The tuning of the NLP spectrum for a pump power of 1.3 W is presented in Figure 5. The tuning range of 35 nm (for peak wavelength), from 1943.5 to 1978 nm, was obtained by adjusting the PC position. A tunable NLP generation in the TDFL mode-locked by a semiconductor saturable absorber mirror (SESAM) with a tuning range of 47 nm has already been presented [17]. However, this setup was not developed in an all-fiber format, and a filter based on chromatic dispersion of lenses was used for wavelength tuning. In our oscillator, NOLM not only acted as an SA, but also enabled wavelength tuning. The adjustment of the PC position inside the loop changed the polarization states and introduced wavelength-dependent losses into the laser cavity. The developed TDFL exhibits continuously tunable NLPs. The 3 dB spectral bandwidth of 12.9–18.5 nm was maintained throughout the tuning range in NLP mode-locking operation. The broadest NLP spectrum with a 3 dB spectral bandwidth of 17.4 nm was centered at a wavelength of 1961.4 nm. Characteristic dips in the generated NLP spectra, from 1910 nm to approximately 1940 nm, could be observed (especially in the green and red spectra). These dips originated from the absorption of water in atmospheric air.

#### 4. Conclusions

In conclusion, we demonstrated bound-state soliton and NLP generation in a figure-of-eight Tm-doped all-fiber laser setup with dispersion compensation. The developed oscillator generated stretched pulses, NLPs, and bounded solitons at a fundamental repetition frequency of 15.795 MHz. Under a pump power of 513 mW, three bound solitons with duration of 1.4 ps and fixed pulse separations of 12.4 ps were observed. For higher pump power levels, the developed oscillator tended to generate NLPs. At the maximum pump power of ~1.6 W, mode-locked NLPs with pulse energy of 2.91 nJ, FWHM spike duration of 509 fs, and 3 dB spectral bandwidth of 18.5 nm were reported. The NLP output spectrum could be tuned by 35 nm, from 1943.5 to 1978 nm, only by adjusting the PC position. To our knowledge, this is the first report of the generation of a tunable NLP in a mode-locked TDFL based on a nonlinear loop mirror saturable absorber. Due to the compact, simple, and all-fiber configuration, the developed oscillator can be a promising source for many applications, e.g., optical communication and material processing.

**Author Contributions:** Conceptualization, M.M. methodology, M.M. and J.S.; software, P.G.; investigation, M.M.; resources, J.M. and P.G.; data curation, M.M. and J.M.; writing—original draft preparation, M.M.; writing—review and editing, M.M., J.M., P.G. and J.S.; visualization, M.M. and J.M.; supervision, M.M.; funding acquisition, M.M. All authors have read and agreed to the published version of the manuscript.

**Funding:** This research was supported by statutory funds of the Institute of Optoelectronics, Military University of Technology (RMN/08-943/2018/WAT).

**Institutional Review Board Statement:** Not applicable.

**Informed Consent Statement:** Not applicable.

**Data Availability Statement:** Data is available on request.

**Acknowledgments:** The authors thank AM Technologies Sp. z o.o. for providing access to their RF spectrum analyzer.

**Conflicts of Interest:** The authors declare no conflict of interest.

#### References

1. Rudy, C.W.; Dignonnet, M.J.; Byer, R.L. Advances in 2- $\mu$ m Tm-doped mode-locked fiber lasers. *Opt. Fiber Technol.* **2014**, *20*, 642–649. [[CrossRef](#)]
2. Sotor, J.; Bogusławski, J.; Martynkien, T.; Mergo, P.; Krajewska, A.; Przewłoka, A.; Strupinski, W.; Sobon, G. All-polarization-maintaining, stretched-pulse Tm-doped fiber laser, mode-locked by a graphene saturable absorber. *Opt. Lett.* **2017**, *42*, 1592–1595. [[CrossRef](#)] [[PubMed](#)]

3. Wang, Y.; Alam, S.; Obratsova, E.D.; Pozharov, A.S.; Set, S.Y.; Yamashita, S. Generation of stretched pulses and dissipative solitons at 2  $\mu\text{m}$  from an all-fiber mode-locked laser using carbon nanotube saturable absorbers. *Opt. Lett.* **2016**, *41*, 3864–3867. [[CrossRef](#)] [[PubMed](#)]
4. Wienke, A.; Haxsen, F.; Wandt, D.; Morgner, U.; Neumann, J.; Kracht, D. Ultrafast, stretched-pulse thulium-doped fiber laser with a fiber-based dispersion management. *Opt. Lett.* **2012**, *37*, 2466–2468. [[CrossRef](#)] [[PubMed](#)]
5. Haxsen, F.; Ruehl, A.; Engelbrecht, M.; Wandt, D.; Morgner, U.; Kracht, D. Stretched-pulse operation of a thulium-doped fiber laser. *Opt. Express* **2008**, *16*, 20471–20476. [[CrossRef](#)]
6. Michalska, M. Dispersion managed thulium-doped fiber laser mode-locked by the nonlinear loop mirror. *Opt. Laser Technol.* **2021**, *138*, 106923. [[CrossRef](#)]
7. Malomed, B.A. Bound solitons in the nonlinear Schrödinger- Ginzburg-Landau equation. *Phys. Rev. A* **1991**, *44*, 6954–6957. [[CrossRef](#)]
8. Akhmediev, N.N.; Ankiewicz, A.; Soto-Crespo, J.M. Multisoliton solutions of the complex Ginzburg-Landau equation. *Phys. Rev. Lett.* **1997**, *79*, 4047–4051. [[CrossRef](#)]
9. Tang, D.Y.; Man, W.S.; Tam, H.Y.; Drummond, P.D. Observation of bound states of solitons in a passively mode-locked fiber laser. *Phys. Rev. A* **2001**, *64*, 033814. [[CrossRef](#)]
10. Zhao, L.M.; Tang, D.Y.; Cheng, T.H.; Tam, H.Y.; Lu, C. Bound states of dispersion-managed solitons in a fiber laser at near zero dispersion. *Appl. Opt.* **2007**, *46*, 4768–4773. [[CrossRef](#)]
11. Wang, P.; Bao, C.; Fu, B.; Xiao, X.; Grellu, P.; Yang, C. Generation of wavelength-tunable soliton molecules in a 2- $\mu\text{m}$  ultrafast all-fiber laser based on nonlinear polarization evolution. *Opt. Lett.* **2016**, *41*, 2254–2257. [[CrossRef](#)] [[PubMed](#)]
12. Wang, P.; Zhao, K.; Gui, L.; Xiao, X.; Yang, C. Self-organized structures of soliton molecules in 2- $\mu\text{m}$  fiber laser based on MoS<sub>2</sub> saturable absorber. *IEEE Photon. Technol. Lett.* **2018**, *30*, 1210–1213. [[CrossRef](#)]
13. Wang, Z.; Li, L.; Wang, D.N.; Le, Z.; Zhang, S.; Cao, S.; Fang, Z. Generation of pulse-width controllable dissipative solitons and bound solitons by using an all fiber saturable absorber. *Opt. Lett.* **2019**, *44*, 570–573. [[CrossRef](#)] [[PubMed](#)]
14. Liu, R.; Wang, T.; Zhao, D.; Lin, P.; Yuan, Q.; Ji, H.; Chen, P.; Zhao, Y. Self-organized structures of bound states in a 2  $\mu\text{m}$  dispersion-managed mode-locked fiber laser. *Appl. Opt.* **2019**, *58*, 6464–6469. [[CrossRef](#)]
15. Rohrmann, P.; Hause, A.; Mitschke, F. Solitons beyond binary: Possibility of fibre-optic transmission of two bits per clock period. *Sci. Rep.* **2012**, *2*, 866. [[CrossRef](#)]
16. Li, L.; Huang, H.; Su, L.; Shen, D.; Tang, D.Y.; Klimczak, M.; Zhao, L.M. Various soliton molecules in fiber systems. *Appl. Opt.* **2019**, *58*, 2745–2753. [[CrossRef](#)]
17. Mashiko, Y.; Fujita, E.; Tokurakawa, M. Tunable noise-like pulse generation in mode-locked Tm fiber laser with a SESAM. *Opt. Express* **2016**, *24*, 26515–26520. [[CrossRef](#)]
18. Li, J.; Zhang, Z.; Sun, Z.; Luo, H.; Liu, Y.; Yan, Z.; Mou, C.; Zhang, L.; Turitsyn, S.K. All-fiber passively mode-locked Tm-doped NOLM-based oscillator operating at 2- $\mu\text{m}$  in both soliton and noisy-pulse regimes. *Opt. Express* **2014**, *22*, 7875–7882. [[CrossRef](#)]
19. Voropaev, V.; Donodin, A.; Voronets, A.; Vlasov, D.; Lazarev, V.; Tarabrin, M.; Krylov, A. Generation of multi-solitons and noise-like pulses in a high-powered thulium-doped all-fiber ring oscillator. *Sci. Rep.* **2019**, *9*, 18369. [[CrossRef](#)]
20. Sobon, G.; Sotor, J.; Martynkien, T.; Abramski, K.M. Ultra-broadband dissipative soliton and noise-like pulse generation from a normal dispersion mode-locked Tm-doped all-fiber laser. *Opt. Express* **2016**, *24*, 6156–6161. [[CrossRef](#)]
21. Michalska, M.; Swiderski, J. Noise-like pulse generation using polarization maintaining mode-locked thulium-doped fiber laser with nonlinear amplifying loop mirror. *IEEE Photon. J.* **2019**, *11*, 1504710. [[CrossRef](#)]
22. Donovan, G.M. Dynamics and statistics of noise-like pulses in mode-locked lasers. *Physica D* **2015**, *309*, 1–8. [[CrossRef](#)]
23. Zaytsev, A.; Lin, C.; You, Y.; Chung, C.; Wang, C.; Pan, C. Supercontinuum generation by noise-like pulses transmitted through normally dispersive standard single-mode fibers. *Opt. Express* **2013**, *21*, 16056–16062. [[CrossRef](#)] [[PubMed](#)]
24. Chang, K.; Chen, W.; Lin, S.; Hwang, S.; Liu, J. High-power, octave-spanning supercontinuum generation in highly nonlinear fibers using noise-like and well-defined pump optical pulses. *OSA Continuum*. **2018**, *1*, 851–863. [[CrossRef](#)]
25. Özgören, K.; Öktem, B.; Yilmaz, S.; Ilday, F.Ö.; Eken, K. 83 W, 3.1 MHz, square-shaped, 1 ns-pulsed all-fiber-integrated laser for micromachining. *Opt. Express* **2011**, *19*, 17647–17652. [[CrossRef](#)]
26. Keren, S.; Horowitz, M. Interrogation of fiber gratings by use of low-coherence spectral interferometry of noiselike pulses. *Opt. Lett.* **2001**, *26*, 328–330. [[CrossRef](#)]
27. Keren, S.; Brand, E.; Levi, Y.; Levit, B.; Horowitz, M. Data storage in optical fibers and reconstruction by use of low-coherence spectral interferometry. *Opt. Lett.* **2002**, *27*, 125–127. [[CrossRef](#)]
28. Stratmann, M.; Pagel, T.; Mitschke, F. Experimental Observation of Temporal Soliton Molecules. *Phys. Rev. Lett.* **2005**, *95*, 143902. [[CrossRef](#)]
29. Goloborodko, V.; Keren, S.; Rosenthal, A.; Levit, B.; Horowitz, M. Measuring temperature profiles in high-power optical fiber components. *Appl. Opt.* **2003**, *42*, 2284–2288. [[CrossRef](#)]
30. Doran, N.J.; Wood, D. Nonlinear-optical loop mirror. *Opt. Lett.* **1988**, *13*, 56–58. [[CrossRef](#)]
31. Duling, I.N.; Chen, C.-J.; Wai, P.K.A.; Menyuk, C.R. Operation of a nonlinear loop mirror in a laser cavity. *IEEE J. Quant. Electron.* **1994**, *30*, 194–199. [[CrossRef](#)]
32. Wang, J.; Liang, X.; Hu, G.; Zheng, Z.; Lin, S.; Ouyang, D.; Wu, X.; Yan, P.; Ruan, S.; Sun, Z.; et al. 152 fs nanotube-mode-locked thulium-doped all-fiber laser. *Sci. Rep.* **2016**, *6*, 28885. [[CrossRef](#)] [[PubMed](#)]

33. Wang, B.S.; Mies, E.W. Advanced Topics on Fusion Splicing of Specialty Fibers and Devices. *Proc. SPIE* **2007**, *6781*, 678130. [[CrossRef](#)]
34. Tang, D.Y.; Zhao, L.M.; Zhao, B.; Liu, A. Mechanism of multisoliton formation and soliton energy quantization in passively mode-locked fiber lasers. *Phys. Rev. A* **2005**, *72*, 043816. [[CrossRef](#)]
35. Tang, D.Y.; Zhao, L.M.; Zhao, B. Soliton collapse and bunched noise-like pulse generation in a passively mode-locked fiber ring laser. *Opt. Express* **2005**, *13*, 2289–2294. [[CrossRef](#)]